NMR Solution Structure of the Peptide Fragment 1−30, Derived from Unprocessed Mouse Doppel Protein, in DHPC Micelles†

Evangelos Papadopoulos,‡ Kamila Oglęcka,‡ Lena Mäler,‡ Jüri Jarvet,‡ Peter E. Wright,§ H. Jane Dyson,§ and Astrid Gräslund*,‡

Department of Biochemistry & Biophysics, The Arrhenius Laboratories, Stockholm University, SE-10691 Stockholm, Sweden, and Department of Molecular Biology and Skaggs Institute for Chemical Biology, The Scripps Research Institute, 10550 North Torrey Pines Road, La Jolla, California 92037

Received July 8, 2005; Revised Manuscript Received October 19, 2005

ABSTRACT: The downstream prion-like Doppel (Dpl) protein is a homologue related to the prion protein (PrP). Dpl is expressed in the brains of mice that do not express PrP, and Dpl is known to be toxic to neurons. One mode of toxicity has been suggested to involve direct membrane interactions. PrP under certain conditions of cell trafficking retains an uncleaved signal peptide, which may also hold for the much less studied Dpl. For a peptide with a sequence derived from the N-terminal part (1−30) of mouse Dpl (mDpl(1−30)) CD spectroscopy shows about 40% α-helical structure in DHPC and SDS micelles. In aqueous solution it is mostly a random coil. The three-dimensional solution structure was determined by NMR for mDpl(1−30) associated with DHPC micelles. 2D ^{1}H NMR spectra of the peptide in $q = 0.25$ DMPC/DHPC bicelles only showed signals from the unstructured termini, indicating that the structured part of the peptide resides within the lipid bilayer. Together with ^2H_2O exchange data in the DHPC micelle solvent, these results show an α-helix protected from solvent exchange between residues 7 and 19, and suggest that the α-helical segment can adopt a transmembrane localization also in a membrane. Leakage studies with entrapped calcein in large unilamellar phospholipid vesicles showed that the peptide is almost as membrane perturbing as melittin, known to form pores in membranes. The results suggest a possible channel formation mechanism for the unprocessed Dpl protein, which may be related to toxicity through direct cell membrane interaction and damage.

Prion proteins are associated with neurodegenerative diseases called spongiform transmissible encephalopathies (TSE) (*1*) occurring in a variety of mammals. The diseases are characterized by the accumulation of a pathological form of the host encoded prion protein (PrP) in the infected mammal's brain (*2*−*4*). Prion diseases are associated with the conversion of the nontoxic cellular form of the prion protein (PrP^C) into the abnormally folded aggregated scrapie isoform (PrP^{Sc}). PrP^C is monomeric and easily digested by proteinase K, while PrP^{Sc} forms highly insoluble aggregates and shows a high resistance to proteolytic digestion (*5*).

The Doppel (Dpl) protein is a homologue related to PrP. It is expressed in the brains of mice that lack expression of PrP and causes neuronal cell death. Accumulating evidence suggests that whereas PrP has a neuroprotective role, Dpl is neurotoxic (*6*−*9*). The causes of Dpl protein toxicity have been ascribed at least partly to oxidative stress and disturbance of the nitric oxide metabolism (*9*). However, other mechanisms of toxicity have also been suggested, which take into account the antagonistic effects of PrP and Dpl in causing toxicity. Such models involve competition for a common ligand which in the case of Dpl binding would induce cell death, or unknown antagonistic functions of PrP and Dpl (*6*) or multimeric pore formation by Dpl giving rise to toxic channels in the ER or cell membrane, which might be made defective by the inclusion of PrP components (*10*).

NMR studies of the solution structure of the mature form of bovine PrP (residues 23−230) in aqueous solution show a disordered N-terminal segment (residues 23−124), and a globular C-terminal domain extending from residue 125 (*11*). A basic sequence (residues 23−28) at the N-terminus, resembling a nuclear localization sequence (NLS), appears to have an important role for the internalization of the PrP via endocytosis in neurons. By mutating one of the Lys residues in the N-terminal NLS-like sequence it was shown that the internalization by endocytosis was completely abolished (*12*). The N-terminal sequence, ranging from residue 23 to around 100, has been shown to be responsible for internalization of the entire prion protein. The cellular trafficking, turnover, and membrane interactions of PrP are believed to be of crucial importance for the infection as well as the structure conversion associated with disease (*13*−*19*). It has been shown that under certain circumstances the signal peptide is not cleaved off from the prion protein, but the association of such forms of the protein with infectivity or toxicity remains unclear (*20*, *21*).

Because of the potential involvement of an intact N terminus in the pathology of PrP, we previously decided to

† This work was supported by grants from the Greek State Scholarships Foundation (I. K. Y.), the Swedish Research Council (Contracts 521-2002-6051 and 621-2004-3328), the European Commission (Contracts HPRN-CT-2001-00242 and QLK3-CT-2002-01989) and the National Institutes of Health (Contract AG21601).

* To whom correspondence should be addressed. E-mail: astrid@dbb.su.se. Tel: +46 8 162450. Fax: +46 8 155597.

‡ Stockholm University.

§ The Scripps Research Institute.

10.1021/bi051313f CCC: $33.50
Published on Web 12/07/2005

Table 1: Amino Acid Sequences of Dpl- and PrP-Derived Peptides from Different Species

		10 20 30
		----:----|----:----|----:----|
MOUSE	Dpl(1-30)	MKNRLGTWWVAILCMLLASHLSTVKARGIK
BOVINE	Dpl(1-30)	MRKHLGGCWLAIVCILLFSQLCSVKARGIK
HUMAN	Dpl(1-30)	MRKHLSWWWLATVCMLLFSHLSAVQTRGIK
SHEEP	Dpl(1-30)	MRKHLGGCWLAIVCVLLFSQLSSVKARGIK
MOUSE	PrP(1-28)	MA--NLGYWLLALFVTMWTDVGLCKKRPKP
BOVINE	PrP(1-30)	MVKSHIGSWILVLFVAMWSDVGLCKKRPKP
HUMAN	PrP(1-28)	MA--NLGCWMLVLFVATWSDLGLCKKRPKP
		30 40 50
		----:----|----:----|----:----|
MOUSE	PrP(23-50)	--KKRPKPGGWNTGGSRYPGQGSPGGNRYP

study an N-terminal segment of PrP and its interaction with bilayer membranes. We could observe that the N-terminal part (residues 1−28) of the mouse PrP (mPrP(1−28)), including the signal sequence, functions as a cell penetrating peptide (CPP), able to facilitate the transport of large hydrophilic cargoes through a cell membrane (*22*). It was further demonstrated that the peptide could adopt a wide range of secondary structures, ranging from α-helical in neutral vesicles to mostly *β*-sheet structure in negatively charged vesicles (*22*). Recently an NMR solution structure of the bovine N-terminal (1−30) fragment of PrP (bPrP(1−30)) associated with DHPC micelles was determined, and the α-helical form of the peptide was suggested to reside orthogonal to the phospholipid bilayer in bicelles (*23*).

The structure of the mouse Dpl protein, which has a 23% identity to PrP in the primary structure, but has 179 amino acids instead of 254 for mPrP, has revealed a similar overall topology to that of PrP. The globular C-terminal parts have similar folded structures, whereas the N-terminal parts are largely unstructured in both cases (*24*). In the case of Dpl, the N-terminal part lacks both the octarepeat region and the hydrophobic region around residue 120 which are present in PrP. Like PrP the mature Dpl is expressed on the cell surface and anchored there with a glycosylphosphatidylinositol moiety (*25*), and Dpl also contains a basic sequence at the N-terminus (*25*−*30*). Much less is known about the cell trafficking of Dpl than of PrP, but in view of their homologous properties it is not unlikely that also Dpl under certain conditions may appear in an unprocessed form containing the signal peptide. Since the intriguing antagonism of the PrP and Dpl proteins may have a basis in their membrane interactions, we decided to study the segment of Dpl that corresponds to the unprocessed N-terminus of PrP, and its properties in a membrane-mimicking environment. We also compare their membrane perturbation potencies in terms of causing leakage from liposomes and conclude that mDpl(1−30) is indeed a highly potent inducer of leakage in model membranes.

In the present study we have investigated the structure and membrane-interaction properties of the peptide containing 30 amino acid residues derived from the mouse Dpl protein (mDpl(1−30)). Table 1 shows the sequence of this peptide, and the corresponding sequence of mPrP(1−28), as well as some variants from other species. We discuss the structure similarities and differences between the Dpl peptide and the corresponding peptides derived from bovine and mouse PrP in a DHPC micellar solvent, mimicking a membrane environment.

MATERIALS AND METHODS

Sample Preparation. The peptides melittin, mouse Doppel peptide mDpl(1−30) derived from the mouse Dpl protein, and mouse prion peptides mPrP(1−28) and mPrP(23−50) from the mouse PrP protein were obtained from Neosystem Laboratories (Strasbourg, France; immunograde purity) and used without further purification. The peptide concentration was determined by light absorption on a CARY 4 spectrophotometer with a theoretically calculated molar absorptivity of Trp of 5500 M^{-1} cm^{-1} at 280 nm. Nondeuterated dihexanoyl-*sn*-glycero-3-phosphatidylcholine (DHPC) and deuterated dihexanoyl-*sn*-glycero-3-phosphatidylcholine-d_{22} (DHPC-d_{22}), 1,2-dimyristoyl-d_{54}-*sn*-glycero-3-phosphocholine (DMPC-d_{54}), 1-palmitoyl-2-oleoyl-*sn*-glycero-3-phosphocholine (POPC), and 1-palmitoyl-2-oleoyl-*sn*-glycero-3-[phospho-*rac*-(1-glycerol)] sodium salt (POPG) were purchased from Avanti Polar Lipids Inc. (Alabaster, AL). Deuterated SDS-d_{25} was purchased from Cambridge Isotope Laboratories, Inc. Calcein, a fluorescein derivative, was purchased from Molecular Probes, The Netherlands (Product No. C-481). Triton X-100 was obtained from Sigma. Prepacked PD-10 columns, Sephadex G-25 M, were obtained from Amersham Biosciences.

For the ^{1}H NMR experiments, a sample containing 1.5 mM peptide dissolved in 100 mM DHPC-d_{22} was used. 10% ^2H_2O was added for field/frequency lock stabilization. The pH was 3.5. For ^2H_2O exchange measurements a sample prepared in H_2O was freeze-dried for 24 h, and subsequently dissolved in ^2H_2O immediately prior to conducting NMR experiments. Bicelle samples with $q = 0.25$ were prepared by mixing DMPC-d_{54} with water and 10% ^2H_2O. The inhomogeneous mixture was vortexed repeatedly and dissolved by the addition of 1 M DHPC-d_{22} stock solution to a final concentration of 25 mM DMPC-d_{54} and 100 mM DHPC-d_{22}.

CD spectra were recorded for mDpl(1−30) in aqueous solution, or in solvents containing 150 mM SDS or DHPC, or 10 and 40 mM DHPC, and in 2 mM Na phosphate buffer. For comparison, CD measurements were also performed for the mPrP(1−28) peptide derived from the 28 N-terminal amino acid sequence of the mouse PrP in the same solvents.

Large unilamellar vesicles (LUVs) were prepared by dissolving the phospholipids—POPC and POPG in a desired ratio—in chloroform. The chloroform was evaporated using an argon flow, thus leaving a lipid film. Calcein (55 mM) in 50 mM potassium phosphate buffer (pH 7.4) was used to disperse the lipid film during 10 min of vortexing. (The fluorescence of calcein is well self-quenched at 55 mM.) A final concentration of 10 mM lipids was achieved. The dispersion was freeze−thawed five times using liquid nitrogen/hot water and then passed 21 times through two polycarbonate membranes of 100 nm pore size using an Avestin pneumatic actuator. The LUVs were then passed through three Sephadex-G25 columns in order to remove the non-entrapped calcein. The vesicles were diluted with 50 mM potassium phosphate buffer (pH 7.4) to a desired concentration (∼400 μM) and kept on ice when not involved in measurements. They were used directly after preparation.

Peptide-Induced Calcein Leakage from LUVs Studied by Steady-State Fluorescence Spectroscopy. The fluorescence measurements were conducted on a Perkin-Elmer LS 50B luminescence spectrometer with FL WinLab software. The

experiments were run at room temperature in 4 × 10 mm quartz cuvettes. Calcein was excited at 490 nm, and its emission was scanned from 510 to 530 nm at a rate of 250 nm/min. The bandwidth for excitation and emission was 4 nm. Each measurement was averaged over five times, baseline-corrected, and compensated for small differences in peptide concentration. Three series of experiments were done for each peptide.

The calcein entrapping LUVs (POPG:POPC, 2:8) were diluted to a phospholipid concentration of ∼400 μM, and 750 μL was used for each experiment. The peptides were titrated into the sample with an incubation time of 3 min at 20 °C. The vesicles were lysed at the end of each experimental series with 5 μL of 10% (v/v) Triton X-100 to establish the maximum fluorescence intensity corresponding to each preparation.

CD Spectroscopy. The CD measurements were made on a Jasco J-720 CD spectrometer with a 0.05 mm quartz cell or on an Aviv model 202 CD spectrometer with a 2 mm quartz cell. A PTC-343 controller regulated the temperature. CD scans ranging from 5 to 75 °C were performed to check for the temperature dependence of the secondary structure.

NMR Spectroscopy. The two-dimensional ^{1}H NMR measurements were performed on a Varian Inova spectrometer equipped with a triple-resonance probe head operating at 800 MHz ^{1}H frequency or on a Bruker Avance spectrometer operating at 500 MHz equipped with a cryoprobe. Two-dimensional TOCSY spectra (*26*) were recorded with mixing times of 30, 60, and 80 ms, and two-dimensional NOESY spectra (*27*) were recorded with mixing times of 50, 150, and 300 ms. Water suppression was achieved with the WATERGATE pulse sequence (*28*). The spectra were processed with the program Felix (version 2000, Accelrys Inc.). For the ^{2}H exchange experiments a series of TOCSY spectra with mixing times of 30 or 80 ms as well as 1D experiments were performed. The exchange was monitored for 24 h in about 3 h intervals. All 2D NMR experiments were performed at 45 °C. A 2D ^{1}H TOCSY spectrum with a mixing time of 80 ms was recorded for 1 mM mDpl(1−30) in a $q = 0.25$ bicelle solution.

Diffusion measurements were performed on a Bruker Avance 400 MHz spectrometer as well as on a Varian Inova 600 MHz spectrometer, using a pulsed field gradient spin−echo experiment (*29*). To correct for inhomogeneities in the gradient, a distribution function was included for the gradient, a procedure which significantly improves the accuracy of the diffusion coefficients as previously described (*30*). To avoid flow convection effects, the measurements were carried out at a lower temperature (25 °C) as compared to the 2D ^{1}H NMR experiments. The diffusion coefficient derived from this data was used in combination with the Stokes−Einstein relation to calculate an approximate aggregate radius size. For a simple sphere of radius R the linear translational diffusion is given by

$$D = \frac{kT}{6\pi\eta R}$$

where k is the Boltzmann constant and η is the dynamic viscosity of the medium. A hydration shell of 2.8 Å was assumed for the aggregates. To test the effect of the micelles on the peptide, a 100 mM DHPC solution was prepared and divided into two parts. The first sample was used for diffusion measurements of the lipid micelle alone. mDpl(1−30) (1 mM) was added to the other and was used for measuring the diffusion of the peptide and the lipid micelle in the presence of peptide. The same was done with a bicelle solution. Measurements were also performed for the mDpl(1−30) alone in aqueous solution and of the monomeric DHPC at 0.5 mM, which is much lower than the critical micelle concentration. 10% ^2H_2O was added to all samples for field frequency lock stabilization.

Structure Calculation. Distance constraints were generated from quantifying NOESY cross-peak intensities as described earlier (*31*). Cross-peaks were categorized into five different groups, with upper distance limits of 3.0, 3.5, 4.0, 4.5, and 6.0 Å, respectively, based on their intensities. The upper distance limits were normalized against known distances (*32*). A total of 263 distance constraints (93 intra, 89 sequential, and 81 medium range) were obtained from the assigned NOESY spectrum with $\tau_m = 150$ ms. Structures were calculated with the program DYANA (*33*), version 1.5, using torsion angle dynamics. Standard annealing algorithms were used, and a total of 60 structures were calculated. Out of these, 20 structures were selected, based on their target function and constraint violations, to represent the solution structure. The quality of the structure was checked with the program PROCHECK_NMR (*34*). Visual analyses of the solution structures were made with PyMol (version 0_98rc5). The coordinates of the final structure together with the input constraints have been deposited in the PDB under accession code 1Z65. The chemical shifts assignments were deposited in the BMRB database under the deposition code BMRB-6598.

RESULTS

CD Spectroscopy. The structure induction caused by DHPC in mDpl(1−30) was compared to that in mPrP(1−28), for which earlier studies had revealed striking variations in secondary structure depending on conditions (*22*). Figure 1 shows the CD spectra of mPrP(1−28) in water and weak (2 mM, pH 7) phosphate buffer (a) and in 10 mM and 40 mM DHPC (c). The corresponding spectra of mDpl(1−30) are shown in Figure 1, b and d. The CD spectra show that in water mPrP(1−28) is close to random coil secondary structure, whereas there is a somewhat higher structure propensity for mDpl(1−30). In 2 mM phosphate buffer both peptides display a mixed partly α-helical structure. When DHPC is added up to 40 mM, the mPrP(1−28) gradually shifts toward a β-sheetlike CD spectrum (Figure 1c), whereas the mDpl(1−30) remains a stable partial α-helix (Figure 1d). We conclude that the mDpl(1−30) peptide lacks the structure variability of mPrP(1−28). It remains α-helical under a variety of conditions, and this probably reflects its weaker tendency for aggregation with concomitant β-structure induction.

Using CD we investigated the secondary structure of mDpl(1−30) under conditions similar to those used in NMR spectroscopy. Figure 2 shows the CD spectra of 1.33 mM peptide in an aqueous solvent with 150 mM DHPC, and also includes CD spectra recorded for less concentrated peptide in water and in 150 mM SDS. Also under these conditions there is α-helical structure to around 40% in DHPC, as well as in SDS solvents. The structures are stable in the temperature range from 5 to 75 °C (data not shown).

NMR Spectroscopy and Structure Calculation. We chose to study the mDpl(1−30) structure in a DHPC micelle

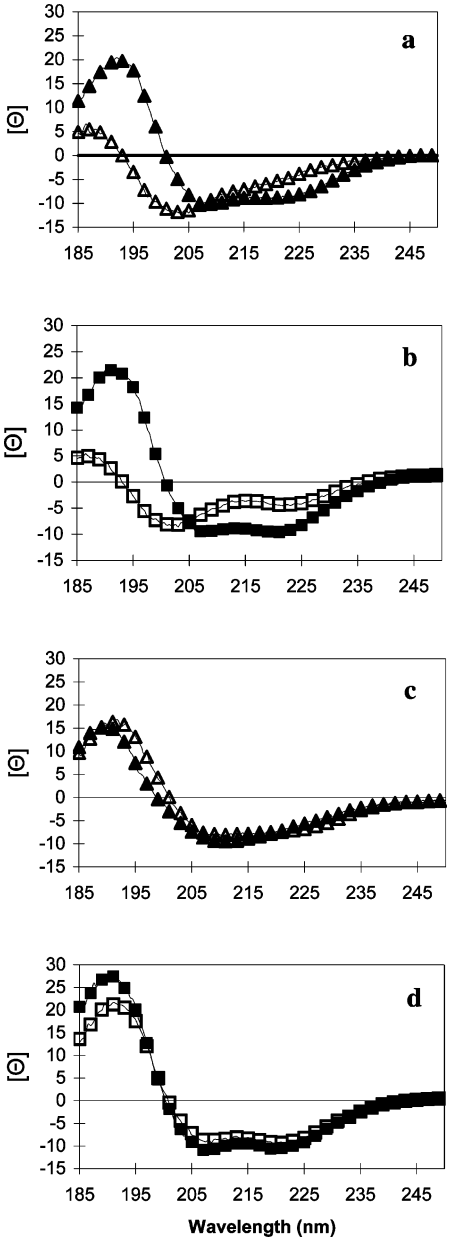

FIGURE 1: CD spectra recorded at 20 °C: [a] (△) 40 μM mPrP(1−28) in water, (▲) 40 μM mPrP(1−28) in buffer; [b] (□) 40 μM mDpl(1−30) in water, (■) 40 μM mDpl(1−30) in buffer; [c] (△) 40 μM mPrP(1−28) in 10 mM DHPC in buffer, (▲) 40 μM mPrP(1−28) in 40 mM DHPC in buffer; [d] (□) 40 μM mDpl(1−30) in 10 mM DHPC in buffer, (■) 40 μM mDpl(1−30) in 40 mM DHPC in buffer. [Θ] is the mean residual molar ellipticity, with the dimension [mdeg cm^{-2} dmol^{-1}]. The buffer was 2 mM Na phosphate buffer, pH 7.0.

environment. The NMR spectra in DHPC micelles had sufficient quality to yield sequence specific assignments using standard procedures. The NMR spectra observed in SDS micellar solvent were less well resolved. For the peptide in DHPC solvent, chemical shifts for the backbone protons were obtained for all residues, except Met1 and the majority of the side-chains were assigned. The secondary chemical shifts for the H$^{\alpha}$ protons, calculated according to ref *35*, indicated an α-helical central part between residues Thr7 and Ser19 (Figure 3), corresponding to 43% helical content. This is in good agreement with the estimate from the CD spectrum obtained under similar conditions (Figure 2).

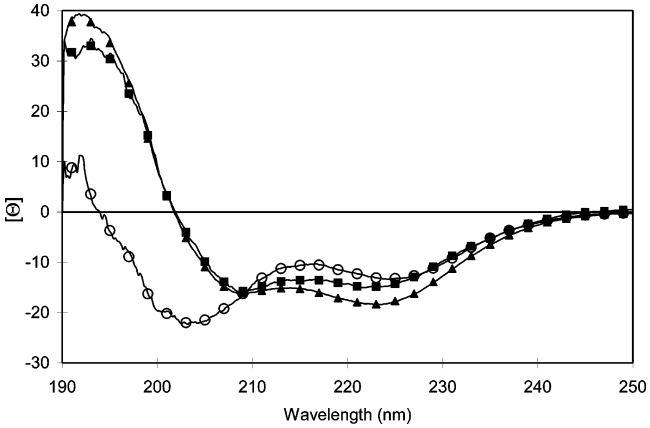

FIGURE 2: CD spectra recorded for mDpl(1−30) at 25 °C: (○) 150 μM mDpl(1−30) in H_2O; (■) 1.33 mM mDpl(1−30) in 150 mM DHPC at 5 °C; (▲) 84 μM mDpl(1−30) in 150 mM SDS. [Θ] is the mean residual molar ellipticity, with the dimension [mdeg cm^{-2} dmol^{-1}].

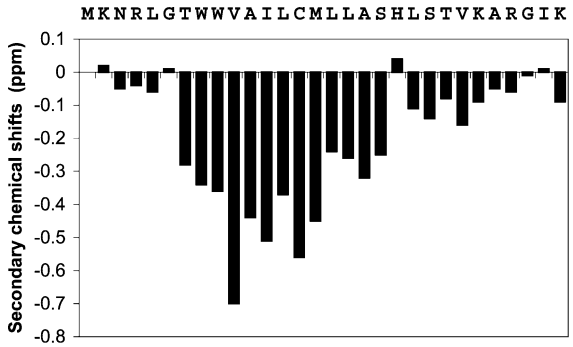

FIGURE 3: Experimental secondary chemical shifts for the H$^{\alpha}$ protons, calculated according to ref *35*, of mDpl(1−30) in 150 mM DHPC solvent.

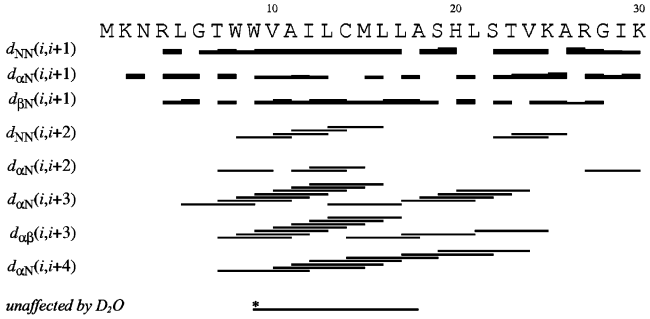

FIGURE 4: Summary of inter-residue constraints used in the structure calculation for mDpl(1−30) derived from a 2D NOESY spectrum with τ_{mix} = 150 ms. The residues for which H^{N}−H$^{\alpha}$ cross-peak intensities are unaffected in the D_2O exchange experiments are also displayed.

From the assigned cross-peaks in the NOESY spectrum, 263 distance constraints were generated and used in the structure calculation. Figure 4 shows a summary of the inter-residue connectivities. The structure, as represented by an ensemble of the 20 best structures, is shown in Figure 5, and the structural statistics are collected in Table 2. Based on analyses of backbone torsion angles and hydrogen bonding patterns, it can be concluded that a helical structure is seen for residues Trp8 through Ser19, again in agreement with the secondary chemical shifts and CD results. It can, however, be noted that there are indications that the helix extends further, both at the N-terminal as well as C-terminal, but that the structure is poorly defined in these regions.

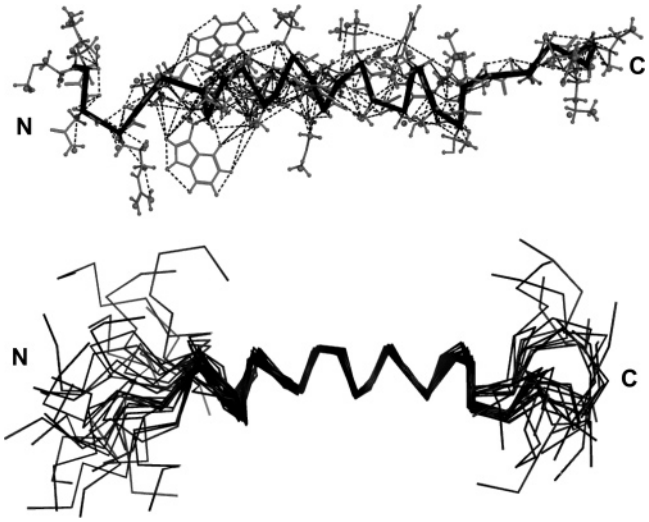

FIGURE 5: The solution structure of mDpl(1−30) in 150 mM DHPC as represented by an overlay of the 20 structures in the ensemble (bottom panel). The overlay was made on the backbone atoms in residues Trp8 − Ser19. The top panel shows an overview of the NOE connectivities used to calculate the structure. The constraints were plotted using the script described at: http://www.pymolwiki.org/index.php/Show_NMR_constrains.

Table 2: Structural Statistics for the Ensemble of 20 mDpl(1−30) Structures in DHPC Micelles Calculated with DYANA

no. of constraints	263
DYANA target function	0.104 ± 0.047 Å^2
max distance violation	0.127 ± 0.030 Å
backbone atom rmsd (Å)	
all residues	2.95
residues 8−21	0.38
Ramachandran plot regions (%)	
most favored	64.0
allowed region	24.0
generously allowed	10.1
disallowed	1.9

Another interesting feature of the NMR ensemble is the localization and position of the tryptophan residues. First of all they are close to the N-terminal end of the α-helix. This would position them close to the polar group interface. Also, as we could clearly assign a few Trp side-chain NOEs, we can see that they are positioned with the plane of the rings parallel to the α-helix axis. Therefore, since the α-helix is orthogonal to the lipid bilayer (see below), so are the Trp side-chains, which is a favorable positioning at the membrane interface. It is notable that Trp residues are present in all Doppel variants (Table 1) and particularly in human Doppel Trp is present in three consecutive copies.

Amide proton exchange experiments were carried out by monitoring the remaining peak amplitudes in a series of TOCSY spectra recorded with a 3-h interval. Part of a TOCSY spectrum recorded after 3 h is shown in Figure 6. The ^2H_2O exchange experiments show that signals corresponding to H^N protons remain for residues Val10 through Ala18 even after 24 h in ^2H_2O at 45 °C. The signals from Trp9 H^N are still visible after 3 h but disappear after 6 h. For the remaining residues, the signals disappear in seconds. This most likely indicates that amide protons for which signals remain are protected from the solvent by the DHPC environment, being located in the hydrophobic interior of the micelle, and shielded from direct contact with the ^2H_2O solvent.

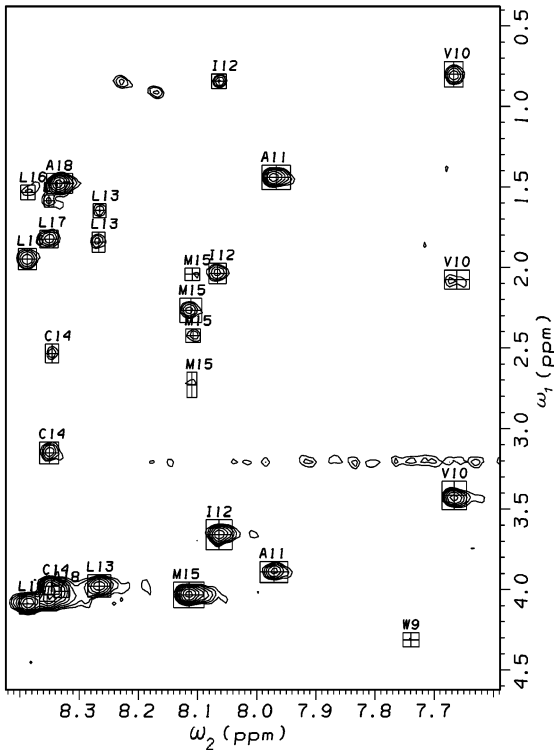

FIGURE 6: Partial 800 MHz TOCSY spectrum ($\tau_{mix} = 80$ ms) of mDpl(1−30) in 150 mM DHPC recorded at 45 °C. The spectrum was recorded 3 h after dissolving in ^2H_2O. Residues Val10 through Ala18 appear unaffected. Residue Trp9 is visible for the first hours, but disappears after 6 h.

Table 3: Summary of Diffusion Measurements at 25 °C[a]

sample	diffusion coefficient (10^{-11} ms^{-2})
mDpl(1−30) in water	16.6
mDpl(1−30) in DHPC micelles	8.9
mDpl(1−30) in $q = 0.25$ bicelles	7.5
monomeric DHPC (0.5 mM)	44.1
DHPC in micelles	18.0
DHPC in micelles with mDpl(1−30)	16.5
DHPC in $q = 0.25$ bicelles	11.7
DHPC in $q = 0.25$ bicelles with mDpl(1−30)	10.4
DMPC in $q = 0.25$ bicelles	8.0
DMPC in $q = 0.25$ bicelles with mDpl(1−30)	7.6

[a] The diffusion coefficients are corrected for the viscosity difference of 10% ^2H_2O where most of the measurements were done. "DHPC micelles" solvent means 150 mM DHPC, and "bicelles" solvent means a $q = 0.25$ mixture of DMPC (25 mM) and DHPC (100 mM).

To compare membrane mimicking solvents, 2D ^1H NMR was also carried out for the peptide in $q = 0.25$ bicelle solution. However only H^N-H^α cross-peaks belonging to the unstructured regions could be observed, while those belonging to the central structured stretch were broadened beyond detection. This further supports the conclusion that the central part forms a stable, rigid helical structure protected from solvent also in a bilayer membrane.

Peptide−Lipid Interactions. NMR diffusion experiments were carried out to probe the size of the peptide−micelle complex and any possible change in the DHPC micelle aggregation number caused by association with the peptide. The comparative diffusion measurements of mDpl(1−30), DHPC, and DMPC in various samples are displayed in Table 3. In general all diffusion coefficients measured here have errors of less than a few %. The peptide in water has a

diffusion coefficient of 16.6 ± 0.4 × 10^{-11} ms^{-2} which according to the Stokes−Einstein relation corresponds to a radius of R_H = 14.8 ± 0.4 Å. Using the relation given by (*36*) gives R_H = 15.7 Å, which is close to the hydrodynamic radius expected for a peptide of this size.

The diffusion constant of mDpl(1−30) in DHPC micelles was calculated using various peptide resonances, which were distinctively clear and separated from DHPC proton peaks. The constants were averaged and gave a linear diffusion constant of $D = 8.87 \pm 0.47 \times 10^{-11}$ ms^{-2} for the peptide−DHPC complex. Using the Stokes−Einstein relation for the diffusion of a sphere, we calculated a corresponding hydrodynamic radius of the peptide−DHPC aggregate to be R_H = 27.2 ± 1.4 Å, clearly larger than for the peptide alone. The error estimate is based on the accuracy of the diffusion constant, as determined from multiple experiments, as well as from the value for the viscosity, η = 0.906 ± 0.005 cP, of the medium. The viscosity is derived for a solution containing 5% to 10% ^2H_2O at 25 °C.

Assuming a hydration shell of 2.8 Å, a lipid density of 1100 kg/m^3, and a peptide density of 1300kg/m^3 we get a total micelle volume of 60 nm^3 with the peptide. Subtracting the volume of the peptide yields an apparent micelle size of 56 nm^3. That corresponds to an average micellar molecular weight of 37.3 ± 8.8 kDa or an aggregation number of 78 ± 19 in the presence of the peptide. This is substantially larger than a normal micelle. For DHPC the critical micellar concentration has been reported as 14 mM, and the micelle aggregate has an average weight of 15−20 kDa with a narrow size distribution (*37*). This corresponds to 36 DHPC molecules per micelle.

DHPC has a substantially larger diffusion coefficient than the peptide in the micellar solution, which can be explained by the assumption that there is always some free monomeric DHPC, diffusing much faster than the peptide−micelle aggregate. We can conclude that for the most part the diffusion for DHPC is affected by the monomeric DHPC concentration. Yet we can qualitatively see the effect of the peptide in the micelle from observing a decrease in the diffusion coefficient, which indicates an increase in the micelle size.

Diffusion was also measured for mDpl(1−30) in q = 0.25 bicelles. From inspecting Table 3 we see that the peptide and DMPC have very similar diffusion coefficients, the same within the experimental error, while DHPC diffuses on average faster. This is due to the fact that a substantial fraction of DHPC exists as monomer in solution (*38*, *39*), while all of the DMPC is bicelle-bound. This shows that more or less all peptide is bound to the bicelle particle. From the DMPC diffusion coefficient we estimate a particle radius of 32.9 ± 3.3 Å. If we take into account the ratio of [DMPC]/[DHPC] = 0.25 and assume a similar density for the two lipids and take into account their molecular weights, we conclude that on average the bicelle consists approximately of 27 molecules of DMPC and 109 molecules of DHPC wrapped around the peptide.

Figure 7 shows the structured peptide enclosed in a modeled DHPC micelle. The diameter of this aggregate agrees well with that determined from the diffusion data, as also determined from the specific volume estimation above. We conclude that the peptide is enclosed by a DHPC micelle. The micelle however may be more accurately modeled as a barrel with the peptide in the interior acting as a nucleation center and the DHPC molecules arranged cylindrically around it. The diameter of this DHPC micelle is around 50 Å. Still, the overall picture of a peptide for which the most hydrophobic segment is enclosed by the hydrophobic part of the lipid chains should be a realistic one.

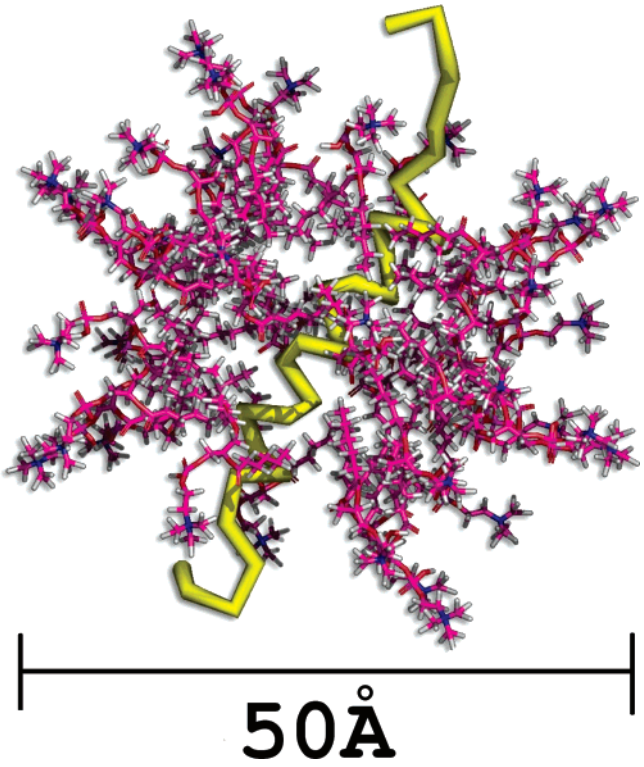

FIGURE 7: Model of the peptide α-helix surrounded by DHPC molecules, consistent with amide proton exchange and diffusion data.

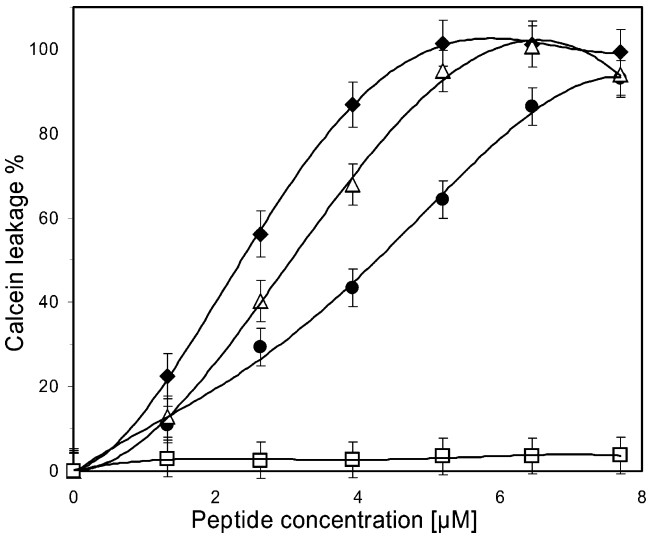

FIGURE 8: Calcein leakage from POPC/POPG (8:2) LUVs caused by addition of mDpl(1−30) (△), mPrPp(1−28) (●), mPrPp(23−50) (□), and melittin (◆) measured by fluorescence spectroscopy. 100% leakage is defined as the measured value after lysing the calcein entrapped vesicles with 5 μL of 10% (v/v) Triton X-100. Lines to guide the eye were obtained by polynomial fitting.

Membrane Leakage Studies. Figure 8 shows the membrane perturbation caused by mDpl(1−30), mPrPp(1−28), mPrPp-(23−50), and melittin. Melittin, included as a reference, is a potent toxic peptide known to form pores in membranes.

It is clear that mDpl(1−30) is even more potent than mPrP-(1−28) in causing leakage of calcein from large unilamellar vesicles (LUVs) composed of phospholipids with a fraction of negatively charged headgroups (POPC with 20% POPG). On the other hand mPrP(23−50), the N-terminus of the progressively processed PrP, causes no leakage even at higher concentrations.

DISCUSSION

The existence of an unprocessed signal peptide has been shown under certain conditions for PrP (*40*). The existence of a corresponding form of the Dpl protein has not been reported, but since its cell trafficking pathways are similar to PrP we may expect this form to appear also for Dpl. The present study deals with the properties of these unprocessed segments. They should be considered as extensions of the N-termini of the proteins, which are unstructured in aqueous solution and should be free to interact with membranes in a cell environment.

The NMR structure of mDpl(1−30) peptide associated with DHPC micelles is, under similar conditions, similar to that of the bPrP(1−30) peptide, derived from the N-terminal sequence of the bovine PrP (*23*). bPrP(1−30) is suggested to act as a cell-penetrating peptide, and may be responsible for the internalization of the entire protein. Interestingly, the peptide derived from the bovine PrP was observed to affect a bilayer membrane in phospholipid bicelles in a way that is characteristic of a transmembrane configuration (*23*). In that case amide proton exchange experiments showed clearly that a central part of the peptide dissolved in DHPC was protected from solvent. In the present study there is a clear similarity between the amide exchange results for the mDpl-(1−30) and bPrP(1−30) peptides. No resonances could be observed for the helical part of either mDpl(1−30) or bPrP-(1−30) in small fast-tumbling bicelles, indicating that both peptides are rigidly attached to the bicelle, with the helical part residing within the bicelle interior. This suggests that also mDpl(1−30) should adopt an orthogonal orientation in a phospholipid bilayer.

These results are in contrast to what has been observed for other helical membrane-interacting peptides, like the typical CPPs penetratin or transportan, which have amphipathic character and reside within the headgroup region in a phospholipid bilayer. For these peptides amide proton exchange occurs within minutes (*41*, *42*). The sequences of both mDpl(1−30) and bPrP(1−30) do not have the characteristics of amphipathic helices, but instead contain quite hydrophobic central regions, with an N-terminal flanking Trp residue (Figure 9). Interestingly, the amphipathic peptides penetratin and transportan gave resolved and assignable spectra in bicelles, and were found to be localized in the headgroup region of the phoshoplipids (*41*, *42*). Although we cannot at this stage give a detailed explanation for the different NMR characteristics, we believe that they have to do with different mobility and exchange properties of a surface-bound peptide compared to a transmembrane peptide.

The diffusion data together with the structure of mDpl-(1−30) provides us with a model for the DHPC−peptide complex (Figure 7). The size of the aggregate indicates that the hydrophobic part of the peptide forms a helix, surrounded by the lipid chains of the DHPC micelle. The indication that the flanking residues at both the N- and C-terminal parts of the helix also have partly helical character suggests that the helix may be longer in a real membrane where the lipid chains are longer.

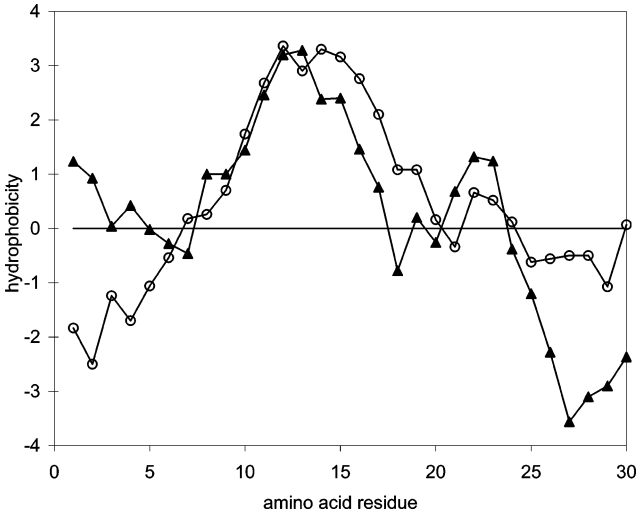

FIGURE 9: Hydrophobicity plot for mDpl(1−30) (○) and bPrP(1−30) (▲), calculated according to ref *44*.

There are notable differences in the membrane interaction between the N-terminal sequences of the PrP and Dpl proteins. The CD results presented here for mDpl(1−30) and mPrP(1−28) (Figure 2) show that the peptide derived from the Dpl protein has a higher propensity for forming stable α-helical structures, as this structure remains under a variety of conditions in terms of peptide/DHPC stoichiometry. The peptide derived from PrP, on the other hand, is seen to have the possibility to form a wider range of structures, including α-helix and *β*-sheet depending on parameters such as peptide/DHPC stoichiometry. For both peptides, the results suggest that membrane interactions of the N-termini of the whole proteins may be important for structuring of the sequences. Formation of a stable α-helix in the N-terminus can be taken to indicate that the corresponding segment is not prone to uncontrolled peptide aggregation, which may be the case when *β*-sheet induction is observed. The observed differences in structure propensity between the N-terminal segments of PrP and Dpl may provide part of the background for their different biological activities, particularly when direct membrane interaction effects are concerned. On the other hand, transmembrane pores formed by well-defined oligomeric aggregates of α-helices are typically associated with membrane-toxic peptides such as melittin derived from bee venom (*43*). In that case the oligomeric, aggregated form of the peptide assembles in the bilayer and forms a channel. A similar situation may occur for the N-termini of unprocessed Dpl proteins interacting with bilayer membranes. This hypothesis is supported by the membrane leakage experiments shown in Figure 8. mDpl(1−30) was found to be almost equally potent as melittin in inducing leakage in LUVs. We conclude that the special combination of fairly hydrophobic signal sequences followed by a highly basic patch is very efficient in causing membrane leakage. These results argue for further cell biology experiments where the trafficking of Dpl is compared with that of PrP and the possible existence of unprocessed Dpl is investigated in experiments where reasons for the observed neurotoxicity are explored.

SUPPORTING INFORMATION AVAILABLE

Animated visualizations of mDpl(1−30) in micelles and bicelles together with the corresponding coordinate files and images of the peptide structure and constraints used. This material is available free of charge via the Internet at http://pubs.acs.org.

REFERENCES

1. Prusiner, S. B. (1997) Prion diseases and the BSE crisis, *Science 278*, 245−251.
2. Prusiner, S. B. (1982) Novel proteinaceous infectious particles cause scrapie, *Science 216*, 136−144.
3. Oesch, B., Westaway, D., Walchli, M., McKinley, M. P., Kent, S. B., Aebersold, R., Barry, R. A., Tempst, P., Teplow, D. B., and Hood, L. E. (1985) A cellular gene encodes scrapie PrP 27−30 protein, *Cell 40*, 735−746.
4. McKinley, M. P., Taraboulos, A., Kenaga, L., Serban, D., Stieber, A., DeArmond, S. J., Prusiner, S. B., and Gonatas, N. (1991) Ultrastructural localization of scrapie prion proteins in cytoplasmic vesicles of infected cultured cells, *Lab. Invest. 65*, 622−630.
5. Prusiner, S. B. (1998) Prions. *Proc. Natl. Acad. Sci. U.S.A. 95*, 13363−13383.
6. Behrens, A., and Aguzzi, A. (2002) Small is not beautiful: Antagonizing functions for the prion protein PrP(C) and its homologue dpl, *Trends Neurosci. 25*, 150−154.
7. Behrens, A. (2003) Physiological and pathological functions of the prion protein homologue dpl. *Br. Med. Bull. 66*, 35−42.
8. Atarashi, R., Nishida, N., Shigematsu, K., Goto, S., Kondo, T., Sakaguchi, S., and Katamine, S. (2003) Deletion of N-terminal residues 23-88 from prion protein (PrP) abrogates the potential to rescue PrP-deficient mice from PrP-like protein/doppel-induced neurodegeneration, *J. Biol. Chem. 278*, 28944−28949.
9. Cui, T., Holme, A., Sassoon, J., and Brown, D. R. (2003) Analysis of doppel protein toxicity, *Mol. Cell. Neurosci. 23*, 144−155.
10. Brini, M., Miuzzo, M., Pierobon, N., Negro, A., and Sorgato, M. C. (2005) The prion protein and its paralogue doppel affect calcium signaling in chinese hamster ovary cells, *Mol. Biol. Cell 16*, 2799−2808.
11. Lopez Garcia, F., Zahn, R., Riek, R., and Wüthrich, K. (2000) NMR structure of the bovine prion protein, *Proc. Natl. Acad. Sci. U.S.A. 97*, 8334−8339.
12. Sunyach, C., Jen, A., Deng, J., Fitzgerald, K. T., Frobert, Y., Grassi, J., McCaffrey, M. W., and Morris, R. (2003) The mechanism of internalization of glycosylphosphatidylinositol-anchored prion protein, *EMBO J. 22*, 3591−3601.
13. Stahl, N., Borchelt, D. R., Hsiao, K., and Prusiner, S. B. (1987) Scrapie prion protein contains a phosphatidylinositol glycolipid, *Cell 51*, 229−240.
14. Prusiner, S. B. (1991) Molecular biology of prion diseases, *Science 252*, 1515−1522.
15. Kocisko, D. A., Come, J. H., Priola, S. A., Chesebro, B., Raymond, G. J., Lansbury, P. T., and Caughey, B. (1994) Cell-free formation of protease-resistant prion protein, *Nature 370*, 471−474.
16. Caughey, B., and Chesebro, B. (2001) Transmissible spongiform encephalopathies and prion protein interconversions, *Adv. Virus Res. 56*, 277−311.
17. Sanghera, N., and Pinheiro, T. J. (2002) Binding of prion protein to lipid membranes and implications for prion conversion, *J. Mol. Biol. 315*, 1241−1256.
18. Kazlauskaite, J., Sanghera, N., Sylvester, I., Venien-Bryan, C., and Pinheiro, T. J. (2003) Structural changes of the prion protein in lipid membranes leading to aggregation and fibrillization, *Biochemistry 42*, 3295−3304.
19. Harris, D. A. (2003) Trafficking, turnover and membrane topology of PrP. *Br. Med. Bull. 66*, 71−85.
20. Fioriti, L., Dossena, S., Stewart, L. R., Stewart, R. S., Harris, D. A., Forloni, G., and Chiesa, R. (2005) Cytosolic prion protein (PrP) is not toxic in N2a cells and primary neurons expressing pathogenic PrP mutations, *J. Biol. Chem. 280*, 11320−11328.
21. Stewart, R. S., and Harris, D. A. (2005) A transmembrane form of the prion protein is localized in the golgi apparatus of neurons, *J. Biol. Chem. 280*, 15855−15864.
22. Lundberg, P., Magzoub, M., Lindberg, M., Hällbrink, M., Jarvet, J., Eriksson, L. E., Langel, Ü., and Gräslund, A. (2002) Cell membrane translocation of the N-terminal (1-28) part of the prion protein, *Biochem. Biophys. Res. Commun. 299*, 85−90.
23. Biverståhl, H., Andersson, A., Gräslund, A., and Mäler, L. (2004) NMR solution structure and membrane interaction of the N-terminal sequence (1-30) of the bovine prion protein, *Biochemistry 43*, 14940−14947.
24. Mo, H., Moore, R. C., Cohen, F. E., Westaway, D., Prusiner, S. B., Wright, P. E., and Dyson, H. J. (2001) Two different neurodegenerative diseases caused by proteins with similar structures, *Proc. Natl. Acad. Sci. U.S.A. 98*, 2352−2357.
25. Silverman, G. L., Qin, K., Moore, R. C., Yang, Y., Mastrangelo, P., Tremblay, P., Prusiner, S. B., Cohen, F. E., and Westaway, D. (2000) Doppel is an N-glycosylated, glycosylphosphatidylinositol-anchored protein. Expression in testis and ectopic production in the brains of Prnp(0/0) mice predisposed to Purkinje cell loss, *J. Biol. Chem. 275*, 26834−26841.
26. Braunschweiler, L., and Ernst, R. (1983) Coherence transfer by isotropic mixing: Application to proton correlation spectroscopy, *J. Magn. Reson. 53*, 521−528.
27. Jeener, J., Meier, B. H., Bachmann, P., and Ernst, R. R. (1979) Investigation of exchange processes by two-dimensional NMR spectroscopy, *J. Chem. Phys. 71*, 4546−4553.
28. Piotto, M., Saudek, V., and Sklenar, V. (1992) Gradient-tailored excitation for single-quantum NMR spectroscopy of aqueous solutions, *J. Biomol. NMR 2*, 661−665.
29. Stejskal, E. O., and Tanner, J. E. (1965) Spin diffusion measurements: Spin echoes in the presence of a time-dependent field gradient, *J. Chem. Phys. 42*, 288−292.
30. Damberg, P., Jarvet, J., and Gräslund, A. (2001) Accurate measurement of translational diffusion coefficients: A practical method to account for nonlinear gradients, *J. Magn. Reson. 148*, 343−348.
31. Andersson, A., and Mäler, L. (2002) NMR solution structure and dynamics of motilin in isotropic phospholipid bicellar solution, *J. Biomol. NMR 24*, 103−112.
32. Wüthrich, K. (1986) *NMR of proteins and nucleic acids*, Wiley, New York.
33. Güntert, P., Mumenthaler, C., and Wüthrich, K. (1997) Torsion angle dynamics for NMR structure calculation with the new program DYANA, *J. Mol. Biol. 273*, 283−298.
34. Laskowski, R. A., Rullmann, J. A., MacArthur, M. W., Kaptein, R., and Thornton, J. M. (1996) AQUA and PROCHECK-NMR: Programs for checking the quality of protein structures solved by NMR, *J. Biomol. NMR 8*, 477−486.
35. Wishart, D. S., and Sykes, B. D. (1994) Chemical shifts as a tool for structure determination, *Methods Enzymol. 239*, 363−392.
36. Danielsson, J., Jarvet, J., Damberg, P., and Gräslund, A. (2002) Translational diffusion measured by PFG-NMR on full length and fragments of the Alzheimer Aβ(1−40) peptide. Determination of hydrodynamic radii of random coil peptides of varying length, *Magn. Reson. Chem. 40*, 89−97.
37. Hauser, H. (2000) Short-chain phospholipids as detergents, *Biochim. Biophys. Acta 1508*, 164−181.
38. Andersson, A., and Mäler, L. (2003) Motilin-bicelle interactions: Membrane position and translational diffusion, *FEBS Lett. 545*, 139−143.
39. Glover, K. J., Whiles, J. A., Wu, G., Yu, N., Deems, R., Struppe, J. O., Stark, R. E., Komives, E. A., and Vold, R. R. (2001) Structural evaluation of phospholipid bicelles for solution-state studies of membrane-associated biomolecules, *Biophys. J. 81*, 2163−2171.
40. Stewart, R. S., Drisaldi, B., and Harris, D. A. (2001) A transmembrane form of the prion protein contains an uncleaved signal peptide and is retained in the endoplasmic reticulum, *Mol. Biol. Cell 12*, 881−889.
41. Bárány-Wallje, E., Andersson, A., Gräslund, A., and Mäler, L. (2004) NMR solution structure and position of transportan in neutral phospholipid bicelles, *FEBS Lett. 567*, 265−269.
42. Lindberg, M., Biverståhl, H., Gräslund, A., and Mäler, L. (2003) Structure and positioning comparison of two variants of penetratin in two different membrane mimicking systems by NMR, *Eur. J. Biochem. 270*, 3055−3063.
43. Bernheimer, A. W., and Rudy, B. (1986) Interactions between membranes and cytolytic peptides, *Biochim. Biophys. Acta 864*, 123−141.
44. Kyte, J., and Doolittle, R. F. (1982) A simple method for displaying the hydropathic character of a protein, *J. Mol. Biol. 157*, 105−132.

BI051313F